Journal of Molecular Catalysis A: Chemical 391 (2014) 99–104

Journal of Molecular Catalysis A: Chemical

journal homepage: www.elsevier.com/locate/molcata

Synergistic effect between orthorhombic α-Sulfur and TiO_2 as co-photocatalysts for efficient degradation of methylene blue: A mechanistic approach

L. Gomathi Devi *, M.L. ArunaKumari

Department of Post Graduate Studies in Chemistry, Central College City Campus, Dr. Ambedkar Street, Bangalore University, Bangalore 560001, India

ARTICLE INFO

Article history:
Received 5 October 2013
Received in revised form 27 January 2014
Accepted 10 April 2014
Available online 19 April 2014

Keywords:
TiO_2
α-Sulfur
Surface sulfation
Non vertical absorption process
Photocatalysis

ABSTRACT

The synergistic effects between α-Sulfur (α-S) and TiO_2 photocatalysts is studied under UV/solar light. An enhancement in photocatalytic activity was observed under UV light, due to formation of sulfate anions in the reaction mixture and these ions get adsorbed on TiO_2 surface by electrostatic force of attraction or it may react with holes/hydroxyl radicals to generate sulfate radical anion. An increase in quantum efficiency is observed with sulfated TiO_2 due to reduction in electron-hole recombination rate. The extended response of α-S under visible region is due to non-vertical absorption process, which paved a new way for elemental photocatalysis.

1. Introduction

Most of the photocatalysts investigated till date are transition metal based compounds like TiO_2, ZnO, WO_3, CdS, ZnS, SnO_2, and Fe_2O_3. Among them TiO_2 is being frequently reported as most active photocatalyst. The photocatalytic activity of TiO_2 is improved by various strategies like coupling with narrow band gap semiconductor, doping of metal/nonmetal ions, codoping with two or more foreign ions, surface modifications by either with organic dyes or with metal complexes, surface fluorination/sulfation/phosphation and noble metal deposition to overcome the drawback of electron–hole recombination and to extend the response to visible region [1–7]. Addition of external oxidants/electron acceptors into a semiconductor suspension have also shown an improvement in photocatalytic degradation by trapping conduction band electron which in turn generates more reactive radicals accelerating the degradation efficiency. However until now, their performance activity has roughly increased by a factor of 2–3 relative to the benchmark Degussa P-25 catalyst [8].

In contrast to overwhelming attention toward compound photocatalysts, recent efforts are made on elemental photocatalysts. In this regard crystalline Silicon, Selenium, Red Phosphorus, α-Sulfur and Boron has gained much attention [9–14]. It is amazing to know that these elemental materials indeed have ability to degrade organic pollutants and they are capable of producing hydrogen from water splitting under visible light by photocatalytic/photoelectrochemical process [15]. Among these elemental materials, Sulfur has attracted the attention because of variety of allotropic forms. A stable configuration of orthorhombic sulfur (α-S) at room temperature is composed of S_8 puckered ring molecule (Fig. 1). α-S is characterized by strong covalent bond between the atoms of the S_8 ring molecule and very much weaker Van der Waals forces binding these atoms together [16,17].

The α-S acts as a photocatalyst under both UV and visible light illumination and generates charge carriers by direct band gap excitation under UV and by non-vertical absorption process under visible light respectively. The poor hydrophilic nature of α-S adds an advantage in its use as a photocatalyst in terms of recycling. In the present work we have reported the synergistic effect of α-S as a photocatalyst along with well known TiO_2 catalyst in various proportions. The reaction mixture is a suspension of solution containing TiO_2 and α-Sulfur particles. Methylene blue (MB) is chosen as model pollutant for photocatalytic degradation.

2. Experimental

2.1. Materials

Titanium (IV) chloride ($TiCl_4 \geq 99.9\%$) is obtained from Merck Chemicals Limited, Methylene Blue (MB) is from Sigma chemical

* Corresponding author. Tel.: +91 09845222867.
E-mail address: gomatidevi_naik@yahoo.co.in (L.G. Devi).

http://dx.doi.org/10.1016/j.molcata.2014.04.012
1381-1169/

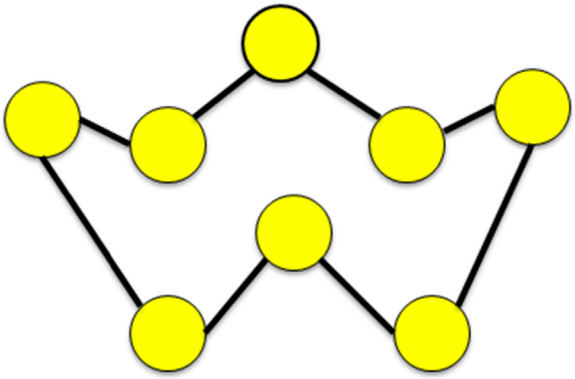

Fig. 1. The puckered ring structure of α-Sulfur.

company, Elemental sulfur from Nice Chemicals Pvt. Ltd., and double distilled water was used throughout the experiment.

2.2. Catalyst preparation

Anatase TiO_2 was prepared by sol–gel method through hydrolysis of $TiCl_4$ as mentioned in earlier literature [18]. 25 mL of diluted $TiCl_4$ was taken along with 1 mL of concentrated H_2SO_4 and diluted to 1 L using double distilled water. Liquor NH_3 was added to the solution to maintain solution pH in range of 7–8. Thus obtained titanium hydroxide gel precipitate was washed several times with double distilled water to remove chloride and ammonium ions completely. The gel was filtered, dried in an oven to remove adsorbed water molecules and then ground to a fine powder, which on calcination at 600○ C for 6 h results anatase TiO_2. α-S is used as received.

2.3. Analytical techniques

The powder X-ray diffraction (PXRD) patterns were obtained using Brucker-D8 advanced diffractometer. The diffraction patterns were recorded using Cu Kα radiation with Ni filter in the specific 2θ range at a scan rate of 2° per min. To study the light absorption characteristics of photocatalysts, absorbance spectra were recorded using Shimadzu-UV 3101 PC UV–VIS–NIR spectrophotometer in range of 200–800 nm. Surface morphology was analyzed by scanning electron microscopic (SEM) analysis using JSM840 microscope operating at 15 kV on specimen upon which thin layer of platinum has been evaporated. FTIR spectra were obtained using Brucker model α-P IR spectrometer with diamond ATR cell.

2.4. Reaction conditions

The photocatalytic activities of TiO_2, α-S and mixture of TiO_2: α-S in various percentage ratio compositions like 75:25 and 50:50 were evaluated by dispersion of 100 mg of catalyst mixture in 250 ml of 10 ppm MB dye solution. The activities of these catalysts were studied under both UV/Solar light irradiation separately. The solution containing the suspension of both TiO_2 and α-S as co-catalysts was stirred in dark for half an hour to reach adsorption equilibrium and then placed under light source with continuous bubbling of air. The degradation reaction was monitored by taking aliquots at regular time intervals and dye concentration was estimated using an UV–vis spectrophotometer by considering difference in absorbance between two aliqots.

3. Results and discussion

3.1. PXRD studies

Fig. 2 shows PXRD patterns of TiO_2 and α-S. The diffraction peaks at 2θ values of 25.3° (1 0 1), 38° (1 1 2), 48° (2 0 0), 54° (1 0 5), 55° (2 1 1), 62° (2 0 4) and 68° (1 1 6) corresponds to anatase phase of TiO_2 (Fig. 2A). The diffraction peaks of α-S (in Fig. 2B) are observed at 2θ values of 15.3° (1 1 3), 23.1° (2 2 2), 25.9° (0 2 6), 26.77° (3 1 1), 27.7° (0 4 0), 28.7° (3 1 3). The numbers in the parenthesis represents hkl values.

The α-Sulfur pattern matches well with standard phase of orthorhombic sulfur (JCPDS Standard 08-0247). The average crystallite sizes of both the catalysts were calculated by using Scherrer's equation:

$$D = \frac{k\lambda}{\beta \cos\theta}$$

where λ is wavelength of Cu Kα source used, β is full width at half maximum (FWHM) of high intense diffraction angle, k is a shape factor (~0.94) and θ is angle of diffraction. The lattice parameters of both samples were determined by using following equation:

$$\frac{1}{d_{hkl}^2} = \frac{h^2}{a^2} + \frac{k^2}{b^2} + \frac{l^2}{c^2}$$

d_{hkl} is distance between (h k l) crystal planes, $h\,k\,l$ is crystal plane index and a, b, c are lattice parameters. The crystallite size, lattice parameters and cell volume of TiO_2 and α-S samples are given in Table 1.

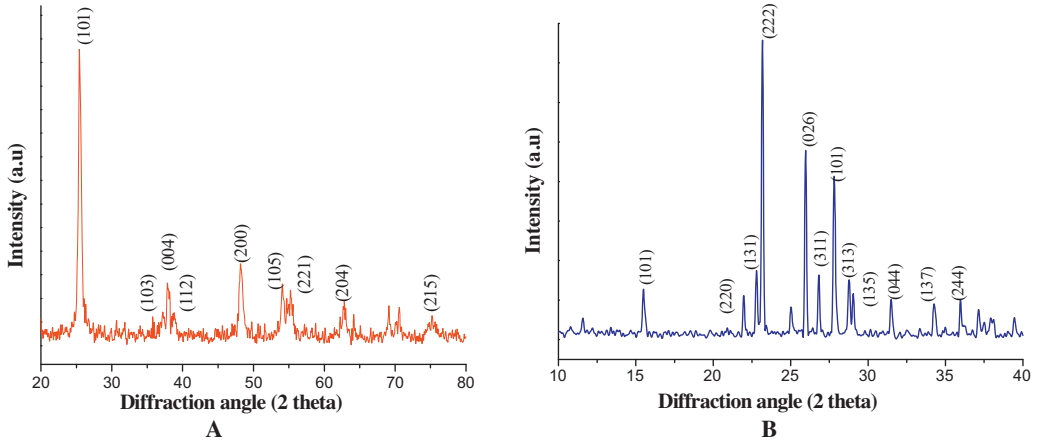

Fig. 2. XRD pattern of (A) TiO_2 and (B) α-Sulfur.

Table 1
Summary of data obtained by X-ray diffraction measurements.

Photocatalyst	Crystallite size D (nm)	Lattice parameters (Å)	Unit cell volume (A°)^3
TiO_2	12.760	$a = b = 3.7836$ $c = 9.5116$	136.16
α-Sulfur	32.479	$a = 10.4560$ $b = 12.8403$ $c = 24.4860$	3287.31

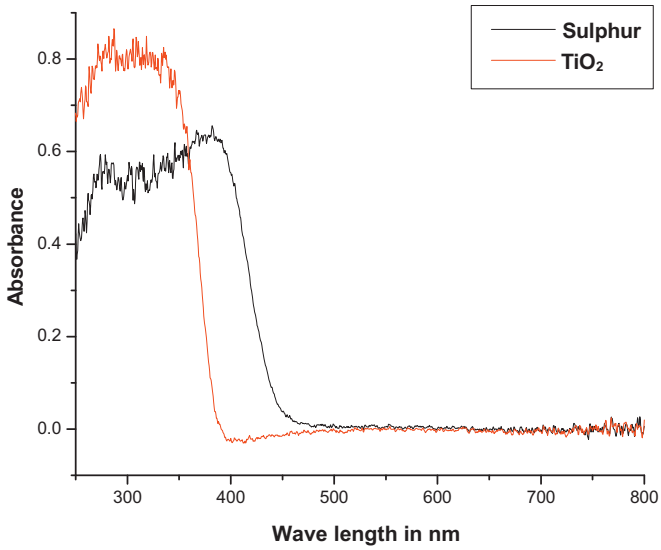

Fig. 3. UV–visible spectra of TiO_2, and α-Sulfur.

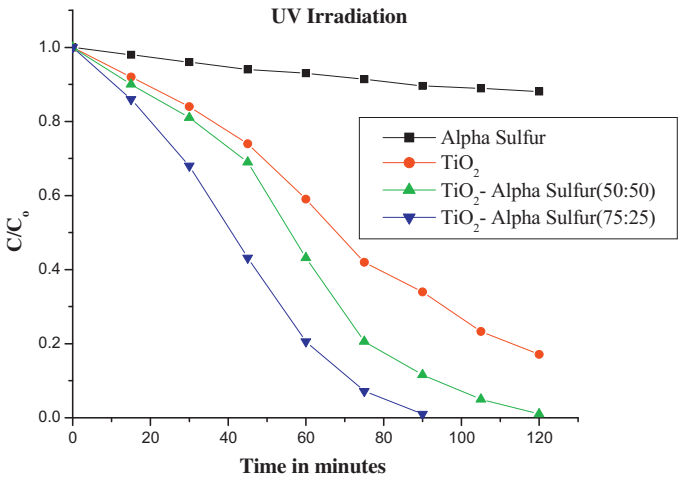

Fig. 5. Plot of C/C_0 versus time under UV illumination for various systems.

3.2. UV–vis absorption spectroscopy

Fig. 3 shows the individual absorption spectra of both TiO_2 and α-S. The absorption spectrum of TiO_2 exhibits a single broad intense absorption peak around 385 nm (corresponding to the band gap of 3.2 eV) involving charge-transfer from valance band (VB), (formed by 2p orbital's of oxygen atoms) to conduction band (CB) (mainly formed by 3d t_{2g} orbital's of Ti^{4+} cations) [19–21]. The extended absorption of α-S in visible-light region around 450 nm was attributed to presence of a trapping level around 2.8 eV above the VB to which electrons could be exited under visible light. These results are in accordance with previous research work by K. K. Thornbert et al. [22].

3.3. Scanning electron microscope (SEM)

Fig. 4A and B shows SEM images of TiO_2 and α-S respectively with significant surface morphology. The surface morphology of TiO_2 was found to be flat and smooth, where as α-S exhibits spherical shape and particles are slightly agglomerated.

3.4. Photocatalytic activity under UV light

Fig. 5 shows plot of C/C_0 versus irradiation time where C and C_0 are residual and initial concentration of MB. Under UV light irradiation, an enhanced photocatalytic activity was observed for 75:25 percentage composition ratio of TiO_2 to α-S. This observed enhancement in degradation reaction can be attributed to the photooxidation of α-S to SO_4^{2-}, which takes place efficiently in presence of anatase TiO_2 under UV light illumination [23]. However it is reported in literature by Matrumdo et al. [23] that

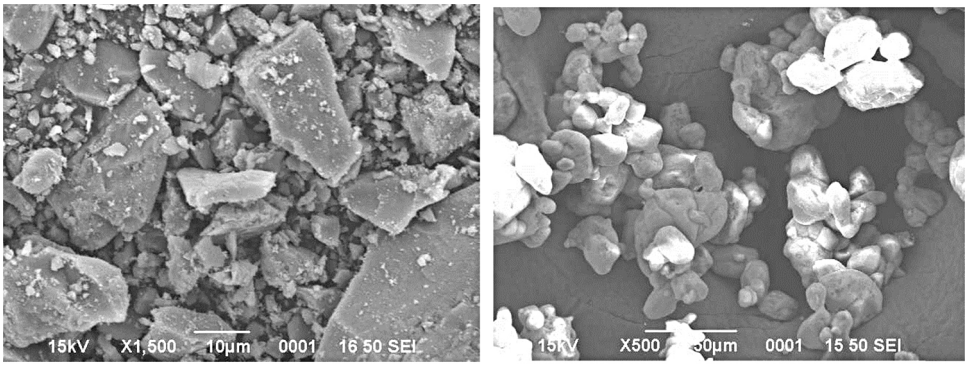

Fig. 4. SEM images of (A) TiO_2 and (B) α-Sulfur.

direct oxidation of sulfur to SO_4^{2-} cannot take place in presence of TiO_2 due to the mismatch of energy levels, whereas M. A. Mendez et al. concluded in their work that the process of oxidation of sulfur to SO_4^{2-} occurs through solvent oxidation. The oxidation of water on TiO_2 generates highly reactive hydroxyl radicals which in turn will oxidize the sulfur to SO_4^{2-} without the need of direct electron transfer between TiO_2 and sulfur [24].

It is well known fact that absorption of photon energy greater than or equal to the band gap of photocatalyst causes charge carrier generation. If charge separation is maintained, thus generated electron and hole may migrate to catalyst surface where they react with adsorbed species, specially holes (h^+) may react with adsorbed H_2O/OH^- to form reactive hydroxide radicals and electrons are trapped by oxygen to generate superoxide radical anions ($O_2^{-\bullet}$) as indicated in following equations:

$$TiO_2 + h\upsilon \xrightarrow{3.2ev} TiO_2(e_{cb}^- + h_{vb}^+) \quad (1)$$

$$(H_2O)_{ads} + h_{vb}{}^+ \rightarrow H^+ + OH^\bullet \quad (2)$$

$$2(OH^-)_{ads} + h_{vb}{}^+ \rightarrow OH^- + OH^\bullet \quad (3)$$

$$O_2 + e_{cb}{}^- \rightarrow O_2{}^{-\bullet} \quad (4)$$

$$O_2{}^{-\bullet} + H^+ \rightarrow HOO^\bullet \quad (5)$$

$$2HOO^\bullet \rightarrow H_2O_2 + O_2 \quad (6)$$

$$H_2O_2 + e_{cb}{}^- \rightarrow OH^- + OH^\bullet \quad (7)$$

The above photogenerated hydroxyl and peroxoradicals in turn take part in various photooxidation reactions with α-S to generate SO_4^{2-} efficiently in aqueous medium since α-S is not stable under UV irradiation [23].

$$\alpha\text{-S} + OH^\bullet \rightarrow \alpha\text{-SOH}^\bullet \quad (8)$$

$$4\alpha\text{-SOH}^\bullet + 4HOO^\bullet \rightarrow H_2S + 6H^+ + 3SO_4^{2-} \quad (9)$$

$$2\alpha\text{-S} + 4HO^\bullet \rightarrow H_2S + 2H^+ + SO_4^{2-} \quad (10)$$

The initial step involves the ring breaking of S_8 molecule and the formation of SO_4^{2-} occurs in subsequent steps and this SO_4^{2-} anion can react in two pathways: (i) it may get adsorbed on surface of TiO_2 due to electrostatic attraction and it can actively participate in trapping of photogenerated electron thereby suppressing e^-–h^+ recombination process. Consequently photogenerated holes promote the formation of hydroxyl radical. Alternatively surface adsorbed SO_4^{2-} anions also affects photocatalytic oxidation process by changing surface charge on TiO_2 surface resulting in better adsorption of MB since it is a cationic dye. (ii) SO_4^{2-} ions may react with holes or hydroxyl radicals leading to generation of sulfate radical anion ($SO_4^{\bullet-}$), which further reacts with water molecules and produces hydroxyl radicals [25,26].

$$SO_4^{2-} + h_{vb}{}^+ \rightarrow SO_4^{\bullet-} \quad (11)$$

$$SO_4^{2-} + HO^\bullet \rightarrow SO_4^{\bullet-} + OH^- \quad (12)$$

$$SO_4^{\bullet-} + H_2O \rightarrow SO_4^{2-} + HO^\bullet + H^+ \quad (13)$$

Sulfate radical anion is one of the strong oxidizing species with a redox potential of 2.6 V similar to that of hydroxyl radical 2.8 V. In addition to its oxidizing strength, sulfate radical anions have several advantages over other oxidants since, it is kinetically fast and it is more stable than hydroxyl radical and capable of migrating longer distances in sub-surface level. It also provides better acidic pH and acts as an efficient electron acceptor in accelerating the mineralization process [27].

However the poor activity of 50:50 mixtures of TiO_2 and α-S was attributed to meager production of SO_4^{2-} ions and it can also be due to poor penetration of UV-light into solution because of hydrophobic suspension of α-S particles. The low density and high hydrophobic nature makes α-S to float above the solution.

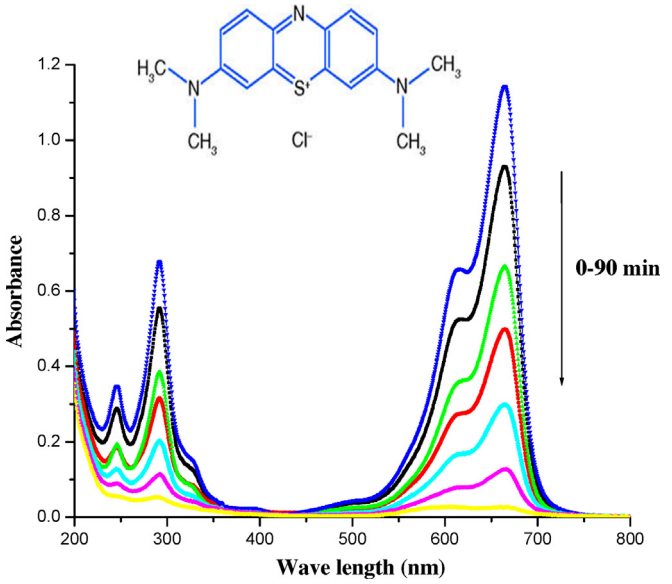

Fig. 6. UV–visible spectra of MB for the photocatalytic degradation reaction recorded at different time intervals. The inset of the figure gives the structure of MB. The experimental conditions are 10 ppm MB + 100 mg of the catalyst mixture containing TiO_2 and α-Sulfur in the ratio 75:25 under UV illumination.

The oxidation of sulfur to sulfate ions in aqueous reaction medium in the presence of TiO_2 under UV light irradiation is tested by measuring conductivity and pH of the solution with respect to time. This allows the reaction to be monitored with a high degree of reproducibility. During course of sulfur oxidation, pH of the solution changes from neutral to acidic and also the conductivity of the aqueous reaction medium increases. This is due to formation of highly conducting SO_4^{2-} ions in the solution. It was observed that, in absence of TiO_2 and UV light oxidation of sulfur did not takes place and no SO_4^{-2} ions were formed even after irradiating the α-S reaction suspension system for many hours. The conductivity decreases when experiment is performed in absence of air bubbling due to poor generation of SO_4^{-2} ions. The results are in accordance with previous report [23].

Absorption spectra of MB show λ_{max} at 663 nm. The benzene chromophore in the MB shows three peaks at 190, 244, 292 nm due to π–π^* transitions which can be designated as E_1, E_2 and B bands. The λ_{max} observed at 663 nm is due to the extended conjugation in the molecule and also due the presence of —C=S, —C=N functional groups. The intensity of all the peaks decreased rapidly with time and it almost disappeared at 90 min time interval. The initial step of degradation can be ascribed to the cleavage of the bonds of the —C=S, —C=N functional groups which can undergo hemolytic cleavage (Fig. 6).

Due to the hydrophobic nature of α-S it floats on the surface of reaction mixture when stirring is completely stopped and it can be separated easily. The TiO_2 which settles at the bottom can be centrifuged and separated. FTIR spectrum (Fig. 7) of TiO_2 separated from α-S in aqueous medium shows sulfate peaks at 1150, 1043, 956 cm^{-1} which are characteristic features of sulfate co-ordinated to TiO_2 in bidentate mode. The peak at 1043 and 956 cm^{-1} corresponds to S—O stretching frequency and peak at 1150 cm^{-1} can be assigned to S=O stretching frequency.

3.5. Photocatalytic activity under solar light

Fig. 8 shows plots of C/C_0 versus irradiation time. In case of visible light irradiation ($\lambda > 400$ nm) α-S shows very good

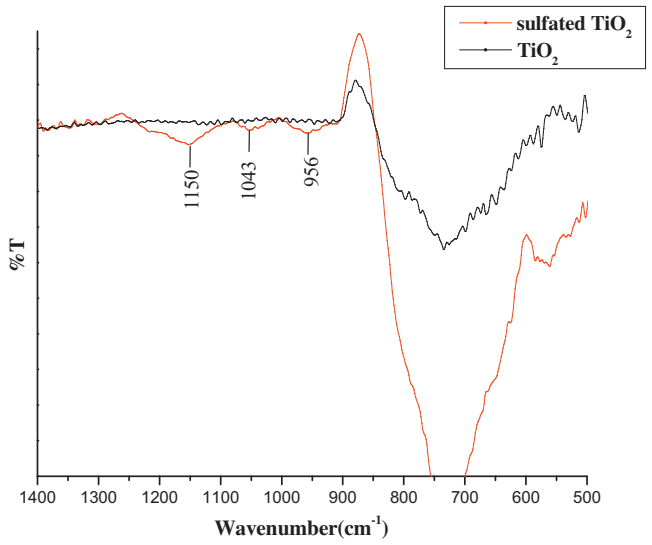

Fig. 7. FTIR spectra of TiO_2 and sulfated TiO_2.

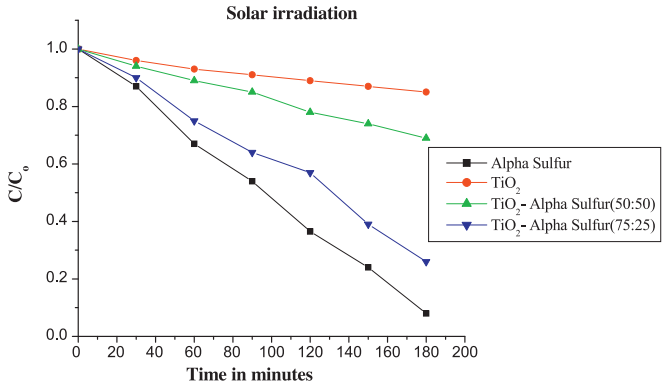

Fig. 8. Plot of C/C_0 versus time under solar light illumination for various systems.

photocatalytic activity compared to composite catalyst (TiO_2: α-S) and pristine TiO_2. This is because α-S shows extended visible light absorption. The much lower activity of TiO_2 is attributed to its large band gap.

The role of α-Sulfur as a visible light photocatalyst can be better understood by considering electronic states of α-S lattice (Fig. 9) as determined from molecular orbital analysis by Dalrymple et al. [28]. According to them, the eight member ring of S_8 is composed of 3s and 3p atomic orbitals, which are sp^3 hybridized to form four molecular orbitals. Among these molecular orbitals, two of them participate in directed bond formation and other two forms equivalent lone-pair orbitals.

This arrangement satisfies the valency of all sulfur atoms involved in ring configuration. The strong overlapping between

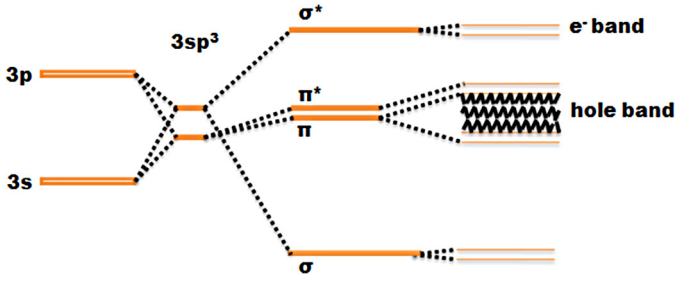

Fig. 9. The electronic states of α-Sulfur lattice.

bonding orbitals will lead to splitting up of these orbitals into bonding and antibonding states. The lone pair orbital's forms molecular π-system which overlaps less strongly. The π and π* energy levels lie fairly close to each other. The band formed from the π–π* states was found to be the highest occupied molecular orbital (HOMO), whereas σ* forms the lowest unoccupied molecular orbital (LUMO). As estimated by Abass et al., the direct band gap of α-Sulfur is ~4.43 eV and an absorption band of α-S in visible-light region is around ~2.79 eV which is an indicative of a non vertical absorption process [17,29]. This is attributed to presence of a trapping level around ~2.8 ev above the VB, to which an electron could be exited generating a hole in VB as reported by Thornber et al. [22]. By drift mobility method Spear et al., determined that at energies below 2.8 eV hole generation remains considerably more efficient than electron generation. But above 2.8 eV, hole generation actually decreases. This is attributed to non vertical process, where excited electrons are propagated by intermolecular electron hopping transport, which shows an excess holes movement in VB [30–32]. Thus available excess holes further generate reactive hydroxyl radicals by solvent oxidation, which in turn degrades the pollutant molecules efficiently.

4. Conclusion

The synergistic effect observed between α-sulfur with TiO_2 as co-catalysts was studied in detail. Under UV-light illumination, the enhanced photocatalytic activity was found for 75:25 percentage composition of mixture containing TiO_2 and α-S. This enhancement in activity of these co-catalysts is attributed to the generation of sulfate ions in reaction mixture and these ions could further react with hole or hydroxyl radical leading to production of sulfate radical anion which is a strong oxidizing species. Simultaneously it may lead to the surface sulfation of TiO_2, which decreases the recombination of photogenerated charge carriers. Under solar light irradiation, α-S exhibits better photocatalytic activity due to the presence of a trapping level around ~2.8 eV above VB, to which electrons could be exited generating a hole in VB, which further generates hydroxyl radicals efficiently by solvent oxidation to enhance the efficiency of degradation reaction.

Acknowledgements

Authors acknowledge the financial assistance from Department of Science and Technology (DST-IDP & DST-SERC) and University Grants Commission (UGC), Government of India.

References

[1] S.G. Kumar, L.G. Devi, J. Phys. Chem. A 115 (2011) 13211–13241.
[2] M. Pelaez, N.T. Nolan, S.C. Pillai, M.K. Seery, P. Falaras, A.G. Kontos, P.S.M. Dunlop, J.W.J. Hamilton, J.A. Byrne, K.O. Shea, M.H. Entezari, D.D. Dionysiou, Appl. Catal. B: Environ. 125 (2012) 331–349.
[3] R. Daghrir, P. Drogui, D. Robert, Ind. Eng. Chem. Res. 52 (2013) 3581–3599.
[4] M.V. Dozzi, E. Selli, J. Photochem. Photobiol. C: Photochem. Rev. 14 (2013) 13–28.
[5] L.G. Devi, R. Kavitha, Appl. Catal. B: Environ. 140–141 (2013) 559–587.
[6] H. Park, Y. Park, W. Kim, W. Choi, J. Photochem. Photobiol. C: Photochem. Rev. 15 (2013) 1–20.
[7] L.G. Devi, M.L. ArunaKumari, Appl. Surf. Sci. 276 (2013) 521–528.
[8] T. Tachikawa, M. Fujitsuka, T. Majima, J. Phys. Chem. C 111 (2007) 5259–5275.
[9] Z. Kang, C.H.A. Tsang, N.B. Wong, Z. Zhang, S.T. Lee, J. Am. Chem. Soc. 129 (2007) 12090–12091.
[10] Z. Kang, Y. Liu, C.H.A. Tsang, D.D.D. Ma, X. Fan, N.B. Wong, S.T. Lee, Adv. Mater. 21 (2009) 661–664.
[11] Y.D. Chiou, Y.J. Hsu, Appl. Catal. B: Environ. 105 (2011) 211–219.
[12] F. Wang, W.K.H. Ng, J.C. Yu, H. Zhu, C. Li, L. Zhang, Z. Liu, Q. Li, Appl. Catal. B: Environ. 111–112 (2012) 409–414.
[13] G. Liu, P. Niu, L. Yin, H.M. Cheng, J. Am. Chem. Soc. 134 (2012) 9070–9073.
[14] G. Liu, L. Yin, P. Niu, W. Jiao, H.M. Cheng, Angew. Chem. 125 (2013) 6362–6365.
[15] G. Liu, P. Niu, H.M. Cheng, ChemPhysChem 14 (2013) 885–892.
[16] B. Meyer, Chem. Rev. 76 (1976) 367–388.

[17] A.K. Abass, N.H. Ahmad, Phys. Stat. Sol. (a) 91 (1985) 627–630.
[18] L.G. Devi, G.M. Krishnaiah, J. Photochem. Photobiol. A: Chem. 121 (1999) 141–145.
[19] K. Nagaveni, M.S. Hegde, G. Madras, J. Phys. Chem. B 108 (2004) 20204–20212.
[20] N. Venkatachalam, M. Palanichamy, V. Murugesan, J. Mol. Catal. A: Chem. 273 (2007) 177–185.
[21] R. Rahimi, E.H. Fard, S. Saadati, M. Rabbani, J. Sol–Gel Sci. Technol. 62 (2012) 351–357.
[22] K.K. Thornbert, C.A. Mead, J. Phys. Chem. Solids 26 (1965) 1489–1495.
[23] Y. Matrumdo, H. Nagal, E. Sato, J. Phys. Chem. 86 (1982) 4660–4664.
[24] M.A. Mendez, A. Cano, M.F. Suarez, Ultrason. Sonochem. 14 (2007) 337–342.
[25] C. Hu, J.C. Yu, Z. Hao, P.K. Wong, Appl. Catal. B: Environ. 46 (2003) 35–47.
[26] A. Houas, H. Lachheb, M. Ksibi, E. Elaloui, C. Guillard, J.M. Herrmann, Appl. Catal. B: Environ. 31 (2001) 145–157.
[27] L.G. Devi, S.G. Kumar, K.M. Reddy, C. Munikrishnappa, J. Hazard. Mater. 164 (2009) 459–467.
[28] R.J.F. Dalrymple, W.E. Spear, J. Phys. Chem. Solids 33 (1972) 1071–1078.
[29] A.K. Abass, A.K. Hasen, R.H. Misho, J. Appl. Phys. 58 (1985) 1640–1642.
[30] A.R. Adams, W.E. Spear, J. Phys. Chem. Solids 25 (1964) 1113–1118.
[31] W.E. Spear, A.R. Adams, J. Phys. Chem. Solids 27 (1966) 281–290.
[32] D.J. Gibbons, W.E. Spear, J. Phys. Chem. Solids 27 (1966) 1917–1925.